CHAPTER 2

Broad-Scale Patterns of Insect and Disease Activity Across the United States From the National Insect and Disease Survey, 2021

Kevin M. Potter and
Jeanine L. Paschke

INTRODUCTION

Forest insects and diseases have widespread ecological and economic impacts on forests in the United States and may represent the most serious threats to the Nation's forests (Logan and others 2003, Lovett and others 2016, Tobin 2015). U.S. law, therefore, authorizes the U.S. Department of Agriculture, Forest Service to "conduct surveys to detect and appraise insect infestations and disease conditions and man-made stresses affecting trees and establish a monitoring system throughout the forests of the United States to determine detrimental changes or improvements that occur over time, and report annually concerning such surveys and monitoring" (FHP 2022). Insects and diseases cause changes in forest structure and function, species succession, and biodiversity, which may be considered negative or positive depending on management objectives (Edmonds and others 2011). Nearly all native tree species of the United States are affected by at least one injury-causing insect or disease agent, with exotic agents, on average, being considerably more severe than native ones (Potter and others 2019a). Additionally, the genetic integrity of several native tree species is highly vulnerable to exotic diseases and insects (Potter and others 2019b).

An important task for forest managers, pathologists, and entomologists is to recognize and distinguish between natural and excessive mortality, a task relating to ecologically based or commodity-based management objectives (Teale and Castello 2011). Impacts of insects and diseases on forests vary from natural thinning to disruption of valued ecosystem processes due to tree mortality, but insects and diseases that kill trees are not necessarily the enemies of forests (Teale and Castello 2011). If disturbances, including insects and diseases, are viewed in their full ecological context, then some amount can be considered "healthy." Disturbances can sustain forest structures (Manion 2003, Zhang and others 2011) by facilitating a sanitation role, culling weak competitors, and releasing resources needed to support the growth of surviving trees (Teale and Castello 2011).

Analyzing patterns of forest insect infestations, disease occurrences, forest declines, and related biotic stress factors is necessary to monitor the health of forested ecosystems and their potential impacts on forest structure, composition, biodiversity, and species distributions (Castello and others 1995). Introduced insects and diseases are of particular concern because they can extensively damage the biodiversity, ecology, and economy of affected areas (Brockerhoff and others 2006, Mack and others 2000). Few forests remain unaffected by invasive species, and their impacts to forest ecosystems are undeniable. These impacts can include wholesale changes in structures and function of ecosystems (Parry and Teale 2011).

Examining insect pest occurrences and related stress factors from a landscape-scale perspective is useful, given the regional extent of many infestations and the large-scale complexity of interactions between host distribution, stress factors, and the development of outbreaks (Holdenrieder and others 2004, Liebhold and others 2013). One such landscape-scale approach is detecting geographic patterns of disturbance, allowing for the identification of areas at greater

How to cite this chapter:

Potter, Kevin M.; Paschke, Jeanine L. 2023. Broad-scale patterns of insect and disease activity across the United States from the National Insect and Disease Survey, 2021. In: Potter, Kevin M.; Conkling, Barbara L., eds. Forest Health Monitoring: national status, trends, and analysis 2022. Gen. Tech. Rep. SRS-273. Asheville, NC: U.S. Department of Agriculture, Forest Service, Southern Research Station: 25–53. https://doi.org/10.2737/SRS-GTR-273-Chap2.

risk of significant ecological and economic impacts, and for selecting locations for more intensive monitoring and analysis. National Insect and Disease Survey (IDS) data (FHP 2022), coordinated by the Forest Service's Forest Health Protection (FHP) program, provide an important source of information on forest disturbances and their causal agents across broad regions. Recent long-term analyses of these data highlight insects as more widely detected agents of mortality compared to diseases, with bark beetles consistently the most important mortality agents across regions and time (Potter and others 2020a). (These results may be somewhat skewed toward insects because the visible signatures of insect damage are easier for IDS surveyors to detect.)

Here, we report the area affected in 2021 by insect and disease mortality and defoliation agents across all 50 States using IDS data collected by the Forest Service and its State partners. We further estimate the percentage of surveyed tree canopy cover area with insect- and disease-related mortality or defoliation within ecoregions across the United States and identify statistically significant geographic hot spots of mortality or defoliation in the conterminous United States (CONUS).

METHODS

Data

The IDS data (FHP 2022) consist of information from low-altitude aerial survey and ground survey efforts by FHP and its partners in State agencies. These data can be used to summarize insect and disease activity by regions in the CONUS, Alaska, and Hawaii (Potter 2012, 2013; Potter and Koch 2012; Potter and Paschke 2013, 2014, 2015a, 2015b, 2016, 2017, 2022; Potter and others 2018, 2019c, 2020b, 2021). The 2021 data collection season was more typical than 2020, when the global COVID-19 pandemic precluded the ability of many State partners and regional Forest Service personnel to conduct aerial survey flights because of risks posed by spending extended periods of time in the confined space of an aircraft. In 2020, a group of forest health specialists worked together to generate new workflows, training materials, and help sessions to address this challenge, including "scan and sketch" methods to outline damage polygons and points directly on base imagery (Hanavan and others 2021). In 2021, however, most data in the IDS data stream were collected using aerial and ground survey methods.

The IDS data identify areas with mortality and defoliation caused by insect and disease activity, although some important forest insects (such as emerald ash borer [*Agrilus planipennis*] and hemlock woolly adelgid [*Adelges tsugae*]), diseases (such as laurel wilt [*Harringtonia lauricola*], Dutch elm disease [*Ophiostoma novo-ulmi*], white pine blister rust [*Cronartium ribicola*], and thousand cankers disease [*Geosmithia morbida*]), and mortality complexes (such as oak decline) have not been not easily detected or thoroughly quantified through aerial detection and other remote sensing methods. (Recent efforts, however, have successfully used remotely sensed data to map damage caused by hemlock woolly adelgid, laurel wilt, and emerald ash borer in urban settings [Abdulridha and others 2018, Hanavan and others 2015, Pontius and others

2017].) Such pests may attack hosts that are widely dispersed throughout forests with high tree species diversity or may cause mortality or defoliation that is otherwise difficult to detect. A visual interpreter might consider a pathogen or insect to be a mortality-causing agent in one location and a defoliation-causing agent in another, depending on the level of damage to the forest in an area and the convergence of other stress factors (such as drought). In some cases, identified agents of mortality or defoliation are actually complexes of multiple agents summarized under an impact label related to a specific host tree species (e.g., "beech bark disease complex" or "yellow-cedar decline"). In other cases, one or more agents (such as ash yellows [caused by the *Candidatus Phytoplasma fraxini* bacterium], ash rust [*Puccinia sparganioides*], and verticillium wilt [*Verticillium albo-atrum*] in ash [*Fraxinus* spp.]) may cause stress to a tree that may ultimately increase its susceptibility to another agent to which the damage is attributed (such as emerald ash borer). Additionally, differences in data collection, attribute recognition, and coding procedures among States and regions can complicate data analysis and interpretation of results. A comparison of aerial survey data by four aerial observers with ground presence/absence observations found the accuracy of aerial survey data exceeded 70 percent, and damage type observations for tree mortality and defoliation had high levels of accuracy, but further showed the accuracy declined for severity estimates and as specificity for observations went from the genus to the species level for tree species and damage agents (Coleman and others 2018).

In 2021, IDS surveys of the CONUS covered about 191.05 million ha of both forested and unforested area (fig. 2.1), of which approximately 131.35 million ha were forested, representing about 41.6 percent of the 315.99-million-ha tree canopy area of the CONUS. This was approximately twice the percentage of tree-canopied area surveyed in 2020 but similar to the amount surveyed in 2018 (46.6 percent) and 2019 (49.2 percent) (Potter and Paschke 2022; Potter and others 2020b, 2021). Meanwhile, about 7.2 percent (5.60 million ha) of Alaska's 77.78 million ha of forest and shrubland was surveyed in 2021, out of a total of 7.35 million ha surveyed across land cover types. This compares to 12.7 percent in 2018, 10.8 percent in 2019, and 2.8 percent in 2020. Finally, surveyors covered about 860 000 ha of Hawaii during 2021. Approximately 564 000 ha of that area had tree canopy cover, or about 65.5 percent of the 861 000 ha total, compared to 69.4 percent in 2018, 63.9 percent in 2019, and 60.3 percent in 2020.

The Digital Mobile Sketch Mapping (DMSM) platform includes tablet hardware, software, and data support processes allowing trained aerial surveyors in light aircraft, as well as ground observers and those using other remote sensing data, to record forest disturbances and their causal agents. Digital Mobile Sketch Mapping enhances the quality and quantity of forest health data while having the potential to improve safety by integrating with remote sensing platforms (FHP 2019). Geospatial data collected with DMSM are stored in the national IDS database. In an important change from the legacy Digital Aerial Sketch Mapping (DASM) approach,

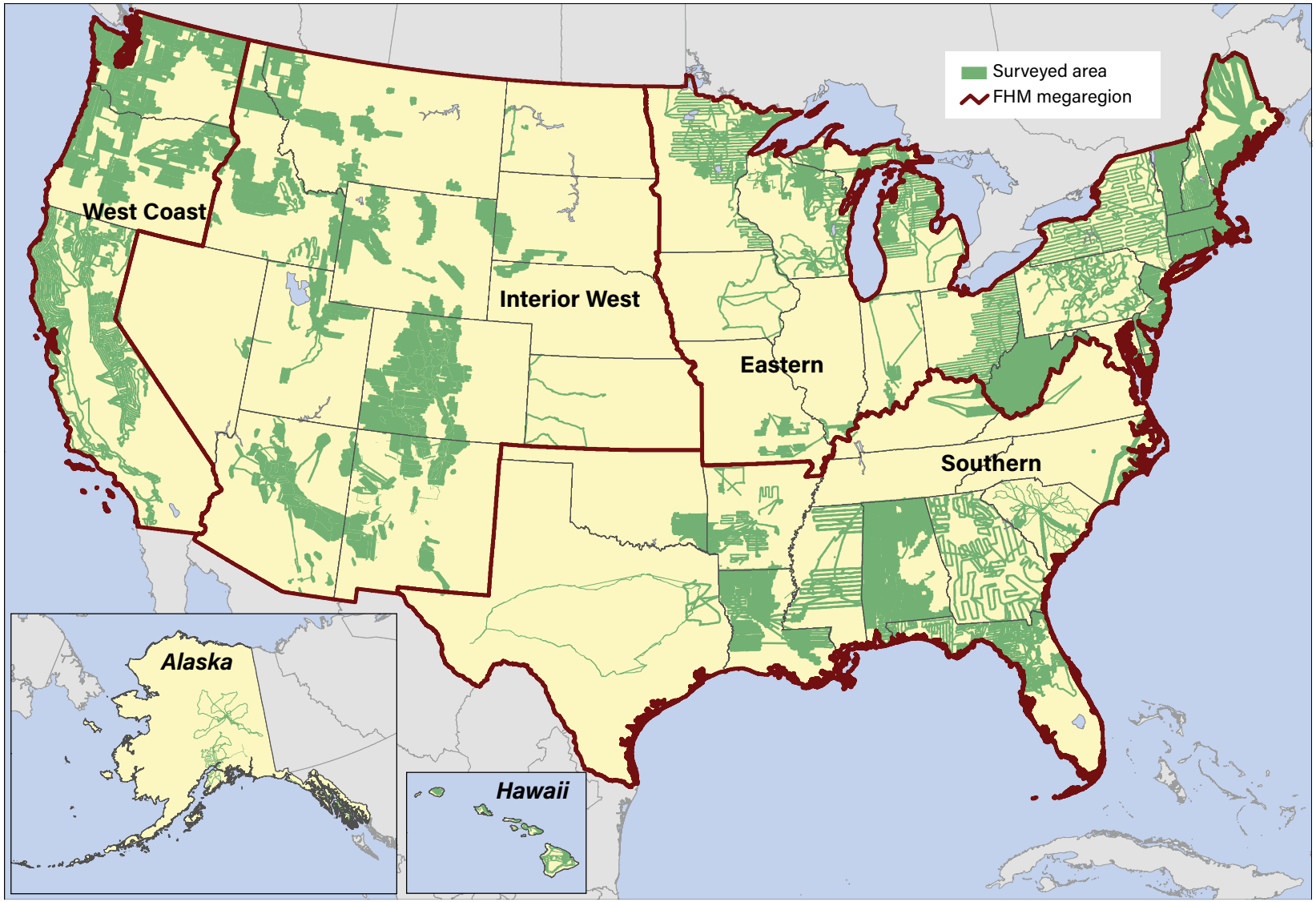

Figure 2.1—The extent of surveys for insect and disease activity conducted in the conterminous United States (CONUS), Alaska, and Hawaii in 2021. The red lines delineate Forest Health Monitoring (FHM) megaregions in the CONUS. Note: Alaska and Hawaii are not shown to scale with map of the CONUS. (Data source: U.S. Department of Agriculture, Forest Service, Forest Health Protection)

the DMSM platform allows surveyors to both define the extent of an area experiencing damage and estimate the percent range of the area within polygons that is affected (Berryman and McMahan 2019). While additional validation is required for this new metric, it should increase the accuracy of derived damage metrics because it potentially corrects for previous overestimation caused by "lassoing" areas of undamaged trees into large areas of damage (Coleman and others 2018, Slaton and others 2021). For this reason, IDS analysis chapters in FHM reports before 2019 did not incorporate derived damage estimates beyond the areal footprint damage with mortality or defoliation polygon boundaries. However, these are now possible because of the inclusion of damage percentage estimates within polygons (see "Analyses" below).

Digital Mobile Sketch Mapping includes both polygon geometry, used for damage areas where boundaries are discrete and obvious, and point geometry, used for small clusters of damage where size and shape of the damage are less important than recording the location. Examples of insects and diseases for which point data are utilized include sudden oak death (caused by the pathogen *Phytophthora ramorum*), southern pine beetle (*Dendroctonus frontalis*), and some types of bark beetle damage in the West. For analyses in this report, these points were assigned an area of 0.8 ha (about 2 acres). Additionally, DMSM allows for the use of grid cells (240-, 480-, 960-, or 1920-m resolution) to estimate the percentage of trees affected by damages that may be widespread and diffuse, such as those associated with spongy moth (*Lymantria dispar*) and emerald ash borer. When calculating the total areas affected by each damage agent, we used the entire areas of these grid cells (e.g., 240-m cell = 5.76 ha).

Analyses

To estimate the extent of damaging insect and disease agents in 2021, we conducted three types of analyses: (1) compiling a series of tables reporting the most widely detected mortality and defoliation agents, (2) describing the percentage of surveyed tree canopy cover area with insect- and disease-related mortality or defoliation within ecoregions across the United States, and (3) using a geographic hot spot analytical approach to identify statistically significant geographic hot spots of mortality or defoliation in the CONUS.

For the first of these, we used the 2021 mortality and defoliation polygons to identify the select mortality and defoliation agents and complexes causing damage on >5000 ha of forest in the CONUS that year. Similarly, we listed the five most widely reported mortality and defoliation agents and complexes within each of the four FHM megaregions in the CONUS (West Coast, Interior West, Eastern, and Southern), as well as for Alaska and Hawaii where data were available. Because of the insect and disease aerial sketch-mapping process (i.e., digitization of polygons by a human interpreter aboard aircraft or by a forest health specialist applying the "scan and sketch" approach with remotely sensed data), all quantities are approximate "footprint" areas for each agent or complex, delineating areas of visible damage within which the agent or complex is present.

Unaffected trees may exist within the footprint, and the amount of damage within the footprint is not reflected in the estimates of forest area affected. The sum of areas affected by all agents and complexes is not equal to the total affected area because of overlapping polygons and the reporting of multiple agents per polygon in some situations.

In our second set of analyses, we used the IDS data for 2021 to more directly estimate impacts of insect- and disease-related mortality and defoliation on U.S. forests. These results are reported in a set of figures describing the percentage of surveyed tree canopy cover area with insect- and disease-related mortality or defoliation within ecoregions across the United States. For these indicators of the extent of damaging insect and disease agents, we summarized the percentage of surveyed tree canopy cover area experiencing mortality or defoliation for ecoregions within the CONUS and Hawaii, and for surveyed forest and shrubland in Alaska ecoregions. This is a change from FHM reports before 2019, in which we reported on the percentage of regions exposed to mortality and defoliating agents based only on the footprint with mortality or defoliation polygon boundaries (masked by forest cover) because information on the percentage of damage within polygons was not yet completely available. As noted above, DMSM now allows surveyors to both define the extent of an area experiencing damage and estimate percent range of the area within the polygon affected (specifically, 1–3 percent, 4–10 percent, 11–29 percent, 30–50 percent, and >50 percent). By multiplying the area of damage within each polygon (after masking by tree canopy cover) by the midpoint of the estimated percent-affected range, it is possible to generate an adjusted estimate of the area affected by each mortality or defoliation agent detection (Berryman and McMahan 2019). These individual estimates can be summed for all polygons within an ecoregion (intersected and dissolved) and divided by the total surveyed tree canopy cover area within the ecoregion to generate an estimate of the percentage of its canopy cover area affected by defoliating or mortality-causing agents. (Digital Mobile Sketch Mapping point data are also included in this estimate. Surveyors have the option to estimate the number of trees affected at a point and are required to assign an area value associated with each point, which is assumed to be 100 percent affected by its mortality or defoliation agent. For simplicity, we transformed each point into a 2-acre [0.809-ha] polygon. These areas for all the points in an ecoregion were then added to the polygon-adjusted affected area estimates for the ecoregion.)

We calculated the percentage of surveyed tree canopy area with mortality or defoliation within each of the 190 ecoregion sections in the CONUS (Cleland and others 2007). Similarly, we summarized mortality and defoliation data for each of the 32 ecoregion sections in Alaska (Spencer and others 2002). For Hawaii, we calculated the percentage of surveyed tree canopy area affected by mortality and defoliation agents in 34 ecoregion subunits on each of the major islands of the archipelago (Potter 2023). We did not calculate statistics for analysis regions in the

CONUS and Hawaii with ≤5 percent of the tree canopy cover area surveyed, nor in Alaska with ≤2.5 percent of the forest and shrubland area surveyed.

We resampled tree canopy data for the CONUS and Hawaii to 240 m from a 30-m raster dataset that estimates percentage of tree canopy cover (0–100 percent) for each grid cell; this dataset was generated from the 2011 National Land Cover Database (NLCD) (Homer and others 2015) through a cooperative project between the Multi-Resolution Land Characteristics Consortium and the Forest Service Geospatial Technology and Applications Center (GTAC) (Coulston and others 2012). For our purposes, we treated any cell with >0-percent tree canopy cover as forest. Comparable tree canopy cover data were not available for Alaska, so we instead created a 240-m-resolution layer of forest and shrub cover from the 2011 NLCD.

Finally, we used the Spatial Association of Scalable Hexagons (SASH) analytical approach to identify statistically significant geographic hot spots of mortality or defoliation in the CONUS. This method identifies locations where ecological phenomena occur at greater or lower frequency than expected by random chance and is based on a sampling frame optimized for spatial neighborhood analysis, adjustable to the appropriate spatial resolution, and applicable to multiple data types (Potter and others 2016). Specifically, it consists of dividing an analysis area into scalable equal-area hexagonal cells within which data are aggregated, followed by identifying statistically significant geographic clusters of hexagonal cells within which mean values are greater or less than those expected by chance. To identify these clusters, we employed a Getis-Ord (G_i^*) hot spot analysis (Getis and Ord 1992) in ArcMap® 10.3 (ESRI 2017) separately for both mortality- and defoliation-causing agents across the CONUS. The low density of survey data in 2021 from Alaska, as well as the small spatial extent of Hawaii (fig. 2.1), precluded the use of Getis-Ord G_i^* hot spot analyses in these areas.

The units of analysis were 9,810 hexagonal cells, each approximately 834 km^2 in area, generated in a lattice across the CONUS using intensification of the Environmental Monitoring and Assessment Program (EMAP) North American hexagon coordinates (White and others 1992). These coordinates are the foundation of a sampling frame in which a hexagonal lattice was projected onto the CONUS by centering a large base hexagon over the region (Reams and others 2005, White and others 1992). This base hexagon can be subdivided into many smaller hexagons, depending on sampling needs, and serves as the basis of the plot sampling frame for the Forest Service's Forest Inventory and Analysis (FIA) program (Reams and others 2005). Importantly, hexagons maintain equal areas across the study region regardless of the degree of intensification of the EMAP hexagon coordinates. In addition, hexagons are compact and uniform in their distance to the centroids of neighboring hexagons, meaning a hexagonal lattice has a higher degree of isotropy (uniformity in all directions) than a square grid (Shima and others 2010). These are convenient and highly useful attributes for spatial neighborhood analyses. These scalable hexagons are independent of geopolitical and

ecological boundaries, avoiding the possibility of different sample units (such as counties, States, or watersheds) encompassing vastly different areas (Potter and others 2016). We selected hexagons 834 km^2 in area because this is a manageable size for making monitoring and management decisions in analyses that are national in extent (Potter and others 2016).

We then used the Getis-Ord G_i^* statistic to identify clusters of hexagonal cells within which the percentage of surveyed tree canopy area with mortality or defoliation was higher than expected by chance. This statistic allows for the decomposition of a global measure of spatial association into its contributing factors, by location, and is therefore particularly suitable for detecting instances of nonstationarity in a dataset, such as when spatial clustering is concentrated in one subregion of the data (Anselin 1992). We excluded hexagons if they contained <5-percent tree canopy cover or if <1 percent of the tree canopy cover was surveyed in 2021.

The Getis-Ord G_i^* statistic for each hexagon summed differences between mean values in a local sample, determined by a moving window consisting of the hexagon and its 18 first- and second-order neighbors (the 6 adjacent hexagons and the 12 additional hexagons contiguous to those 6) and a global mean. The G_i^* statistic was standardized as a *z*-score with a mean of 0 and a standard deviation of 1, with values >1.96 representing significant (p <0.025) local clustering of high values and values <-1.96 representing significant clustering of low values (p <0.025), since 95 percent of observations under a normal distribution should be within approximately two (exactly 1.96) standard deviations of the mean (Laffan 2006). In other words, a G_i^* value of 1.96 indicates the local mean of the percentage of forest exposed to mortality- or defoliation-causing agents for a hexagon and its 18 neighbors is approximately two standard deviations greater than the mean expected in the absence of spatial clustering, while a G_i^* value of -1.96 indicates the local mortality or defoliation mean for a hexagon and its 18 neighbors is approximately two standard deviations less than the mean expected in the absence of spatial clustering. Values between -1.96 and 1.96 have no statistically significant concentration of high or low values. In other words, when a hexagon has a G_i^* value between -1.96 and 1.96, mortality or defoliation damage within it and its 18 neighbors is not statistically different from a normal expectation. As described in Laffan (2006), it is calculated as:

$$G_i^*(\boldsymbol{d}) = \frac{\sum_j w_{ij}(\boldsymbol{d}) x_j - W_i^* \bar{x}^*}{s^* \sqrt{\frac{(n s_{1i}^*) - W_i^{*2}}{n-1}}}$$

where

G_i^* = the local clustering statistic (in this case, for the target hexagon)

i = the center of local neighborhood (the target hexagon)

d = the width of local sample window (the target hexagon and its first- and second-order neighbors)

x_j = the value of neighbor j

w_{ij} = the weight of neighbor j from location i (all the neighboring hexagons in the moving window were given an equal weight of 1)

n = number of samples in the dataset (the 4,303 hexagons containing >5-percent tree cover and with at least 1 percent of the canopy cover surveyed)

W_i^* = the sum of the weights

s^*_{1i} = the number of samples within d of the central location (19: the focal hexagon and its 18 first- and second-order neighbors)

$\overline{x}^*$= mean of whole dataset (in this case, the 4,303 hexagons)

s^* = the standard deviation of whole dataset (for the 4,303 hexagons)

It is worth noting that the -1.96 and 1.96 threshold values are not exact because the correlation of spatial data violates the assumption of independence required for statistical significance (Laffan 2006). The Getis-Ord approach does not require the input data to be normally distributed because the local G_i^* values are computed under a randomization assumption, with G_i^* equating to a standardized z-score that asymptotically tends to a normal distribution (Anselin 1992). The z-scores are reliable, even with skewed data, if the distance band used to define the local sample around the target observation is large enough to include several neighbors for each feature (ESRI 2017).

RESULTS AND DISCUSSION

Conterminous United States Mortality

The national IDS data in 2021 identified 60 mortality-causing agents and complexes across the CONUS on approximately 2.21 million ha, slightly less than the land area of New Hampshire. Of the 60 mortality agents, 13 were detected on >5000 ha within the area surveyed. These numbers were higher than in 2020, when 45 agents and complexes were detected on 1.17 million ha (Potter and Paschke 2022), largely because of the challenges associated with collecting insect and disease damage data during the COVID-19 pandemic. They are more consistent with the numbers during a typical year of data collection, such as 2.69 million ha from 58 agents and complexes in 2019 (Potter and others 2021).

Emerald ash borer was the most widely detected mortality agent in 2021, identified on about 878 000 ha (table 2.1), which represents about 40 percent of the total CONUS mortality area. It is important to note, however, that emerald ash borer damage is challenging to map during aerial surveys, that it is difficult to differentiate the occurrence of damage between years, and that agents other than emerald ash borer affect ash species. Fir engraver (*Scolytus ventralis*), identified on 412 000 ha, was the next most widely detected mortality agent, as in 2020 (Potter and Paschke 2022). Three other agents were detected on >100 000 ha. The first of these is characterized as an "unknown bark beetle" on approximately 230 000 ha, with damage primarily in ponderosa pine (*Pinus ponderosa*) forests by a group of known and varied bark beetles impossible to distinguish using IDS data. This also has been characterized as "Southwest bark beetle complex" consisting mainly of damage caused by roundheaded pine beetle (*D. adjunctus*), western pine beetle (*D. brevicomis*), and ips beetles. As a separate individual agent, western pine beetle was detected on almost 158 000 ha, while eastern larch beetle

Table 2.1—Mortality agents and complexes affecting >5000 ha in the conterminous United States during 2021

Agents/complexes causing mortality, 2021	Area (ha)[a]
Emerald ash borer	877 631
Fir engraver	411 511
Unknown bark beetle[b]	230 426
Western pine beetle	157 550
Eastern larch beetle	101 516
Mountain pine beetle	72 636
Pinyon ips	66 706
Douglas-fir beetle	61 653
Spruce beetle	57 443
Unknown	51 406
Western balsam bark beetle	35 521
Flatheaded fir borer	22 739
Balsam woolly adelgid	18 952
Oak decline	16 832
Jeffrey pine beetle	10 630
Subalpine fir decline	10 104
Ips engraver beetles	7822
Sudden oak death	6578
Other (42)	21 611
Total, all mortality agents	2 213 302

[a] All values are "footprint" areas for each agent or complex. The sum of the individual agents is not equal to the total for all agents due to the reporting of multiple agents per polygon.

[b] In the Interior West, this is primarily damage on ponderosa pines. The group of bark beetles is known and varied but not distinguishable from the air. Regions have characterized it as "Southwest bark beetle complex" consisting mainly of damage caused by roundheaded pine beetle, western pine beetle, and ips beetles.

(*D. simplex)* was identified on 102 000 ha. Meanwhile, mortality from the 14 IDS agents constituting the western bark beetle group (table 2.2) encompassed about 49 percent of all the 2021 mortality area across the CONUS (1.09 million ha in the West).

The Eastern FHM megaregion in 2021 had the largest area on which mortality agents and complexes were detected, about 1.02 million ha (table 2.3), within the surveyed area. The large majority of this (86.2 percent) was associated with emerald ash borer, which was detected on 878 000 ha. Eastern larch beetle was next, at 102 000 ha (10 percent of the total). Oak decline represented 1.7 percent and southern pine beetle was 0.5 percent of the total. Overall, 35 agents and complexes were identified in the megaregion. The ecoregion sections with the greatest mortality of surveyed tree canopy cover were 222M–Minnesota and Northeast Iowa Morainal-Oak Savannah (6.66 percent) and 222L–North Central U.S. Driftless and Escarpment of southwestern Wisconsin, northeastern Iowa, and southeastern Minnesota (5.87 percent), places where emerald ash borer killed white, green, and black ash (*F. americana, F. pennsylvanica*, and *F. nigra*) (fig. 2.2). Parts of these ecoregion sections, along with 251C–Central Dissected Till Plains and 251B–North Central Glaciated Plains, encompassed hot spots of extremely high and very high mortality density (fig. 2.3).

Other ecoregion sections in the Eastern FHM megaregion with relatively high mortality were 212M–Northern Minnesota and Ontario (1.92 percent of surveyed tree canopy cover), following an infestation of eastern larch beetle, and

Table 2.2—Beetle taxa included in the "western bark beetle" group in 2021

Western bark beetle mortality agents	
Douglas-fir beetle	*Dendroctonus pseudotsugae*
Douglas-fir engraver	*Scolytus unispinosus*
Fir engraver	*Scolytus ventralis*
Ips engraver beetles	*Ips* spp.
Jeffrey pine beetle	*Dendroctonus jeffreyi*
Mountain pine beetle	*Dendroctonus ponderosae*
Pine engraver	*Ips pini*
Pinyon ips	*Ips confusus*
Roundheaded pine beetle	*Dendroctonus adjunctus*
Silver fir beetle	*Pseudohylesinus sericeus*
Spruce beetle	*Dendroctonus rufipennis*
Unknown bark beetle	—
Western balsam bark beetle	*Dryocoetes confusus*
Western pine beetle	*Dendroctonus brevicomis*

222I–Erie and Ontario Lake Plain (1.51 percent) because of emerald ash borer-caused mortality in white ash. Both ecoregion sections were locations of hot spots of moderate mortality density (fig. 2.3). Oak decline was an issue in 223B–Interior Low Plateau-Transition Hills (0.49 percent) in south-central Indiana, while eastern larch beetle, emerald ash borer, and eastern spruce budworm (*Choristoneura fumiferana*) all caused mortality in 212T–Northern Green Bay Lobe (0.31 percent).

The West Coast FHM megaregion had the second largest area of detected mortality within the area surveyed, about 748 000 ha linked to 24 agents and complexes (table 2.3). Slightly more than half of this area (53.1 percent) was attributed to fir engraver (397 000 ha). Three other bark beetles were detected on large areas: western pine beetle on 157 000 ha (21.0 percent of the total), mountain pine beetle (*D. ponderosae*) on 66 000 ha (8.8 percent), and Douglas-fir beetle (*D. pseudotsugae*) on 30 000 ha (4.0 percent). Much of eastern and northern California, as well as southwestern Oregon, had at least moderate mortality detected in their surveyed areas (>0.25 percent) (fig. 2.2). First among these ecoregion sections was M261E–Sierra Nevada (1.13 percent), where fir engraver caused mortality in California red fir (*Abies magnifica* var. *shastensis*), mountain pine beetle killed lodgepole pine (*P. contorta*), Jeffrey pine beetle (*D. jeffrey*i) resulted in mortality in Jeffrey pine (*P. jeffreyi*), and western pine beetle affected ponderosa pine stands. Neighboring ecoregion sections also had high mortality: M261D–Southern Cascades (0.94-percent mortality of surveyed areas), M261A–Klamath Mountains (0.93 percent),

Table 2.3—The top five mortality agents or complexes for each Forest Health Monitoring megaregion and for Alaska and Hawaii in 2021

Mortality agents and complexes, 2021	Area (ha)[a]
Eastern	
Emerald ash borer	877 631
Eastern larch beetle	101 516
Oak decline	16 832
Unknown	11 147
Southern pine beetle	4789
Other mortality agents (30)	6171
Total, all mortality agents and complexes	1 018 029
Interior West	
Unknown bark beetle[b]	224 720
Pinyon ips	66 463
Spruce beetle	56 884
Douglas-fir beetle	30 642
Western balsam bark beetle	15 218
Other mortality agents (12)	51 930
Total, all mortality agents and complexes	441 007
Southern	
Ips engraver beetles	2831
Unknown bark beetle[c]	1930
Douglas-fir beetle[c]	1115
Unknown	762
Needlecast	257
Other mortality agents (7)	482
Total, all mortality agents and complexes	6499
West Coast	
Fir engraver	397 297
Western pine beetle	156 989
Mountain pine beetle	65 673
Unknown	36 755
Douglas-fir beetle	29 896
Other mortality agents (19)	81 338
Total, all mortality agents and complexes	747 768
Alaska	
Spruce beetle	78 325
Hemlock sawfly	8510
Yellow-cedar decline	3299
Western balsam bark beetle	36
Aspen running canker	23
Other mortality agents (4)	5
TOTAL	90 196
Hawaii	
Unknown[d]	36 415
Total, all mortality agents and complexes	36 415

[a] The total area affected by other agents is listed at the end of each section. All values are "footprint" areas for each agent or complex. The sum of the individual agents is not equal to the total for all agents due to the reporting of multiple agents per polygon.

[b] In the Interior West, this is primarily damage on ponderosa pines. The group of bark beetles is known and varied but not distinguishable from the air. Regions have characterized it as "Southwest bark beetle complex" consisting mainly of damage caused by roundheaded pine beetle, western pine beetle, and ips beetles.

[c] Personnel from Forest Service Region 3 (Southwestern Region) conducted surveys into southwestern Texas (Region 8 [Southern Region]) because of extended damage in the Guadalupe Mountains which included Douglas-fir beetle and "unknown bark beetle" damage on ponderosa pines (see note b in table 2.1).

[d] Most of the mortality recorded in Hawaii is coded as "unknown" mortality on ʻōhiʻa lehua. Damage is likely attributed to rapid ʻōhiʻa death but has not been confirmed in all cases.

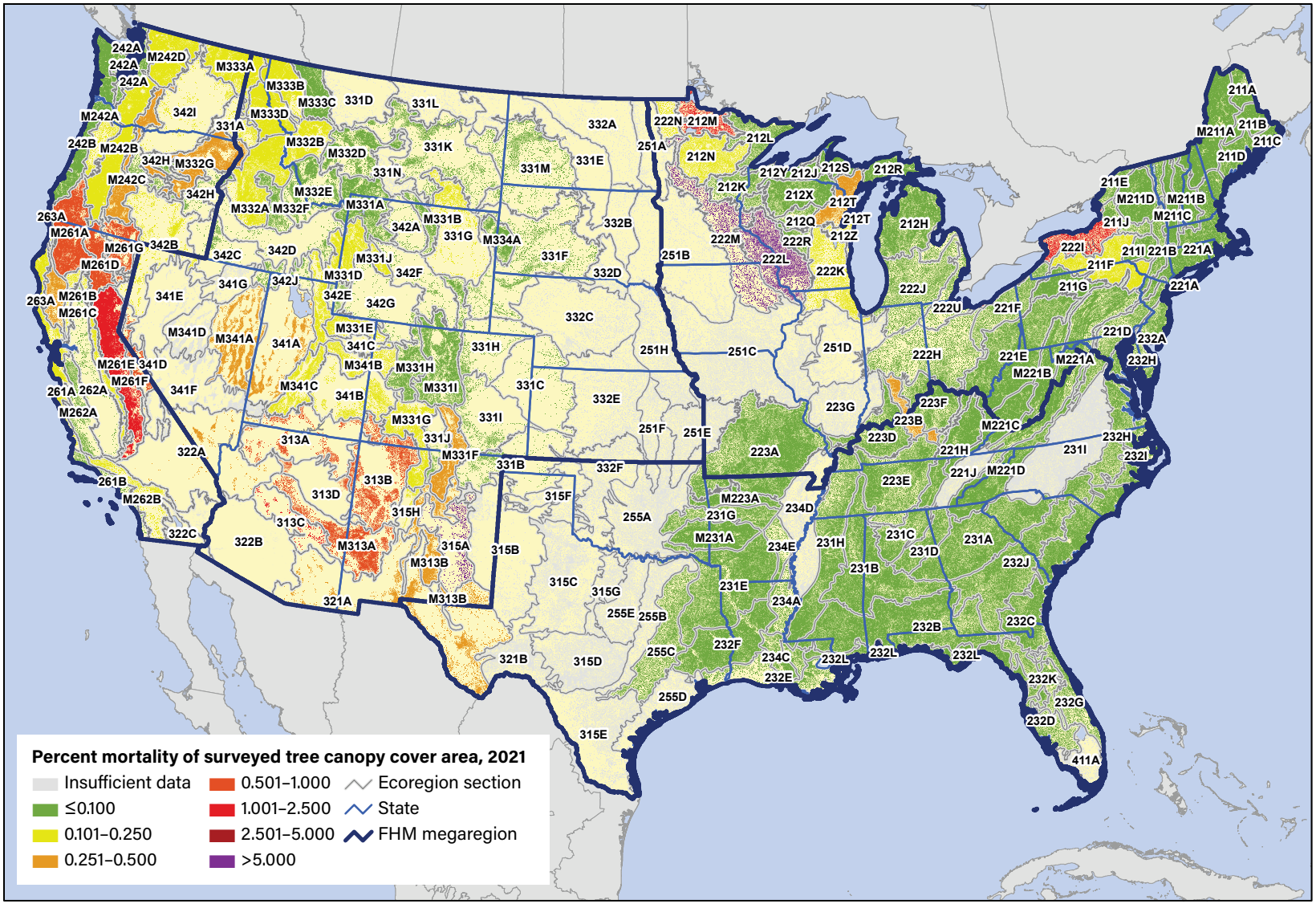

Figure 2.2—The percentage of surveyed tree canopy cover area with insect and disease mortality, by ecoregion section within the conterminous United States, for 2021. The gray lines delineate ecoregion sections (Cleland and others 2007), and blue lines delineate Forest Health Monitoring megaregions. The 240-m tree canopy cover is based on data from a cooperative project between the Multi-Resolution Land Characteristics Consortium (Coulston and others 2012) and the Forest Service Geospatial Technology and Applications Center using the 2011 National Land Cover Database. (Data source: U.S. Department of Agriculture, Forest Service, Forest Health Protection)

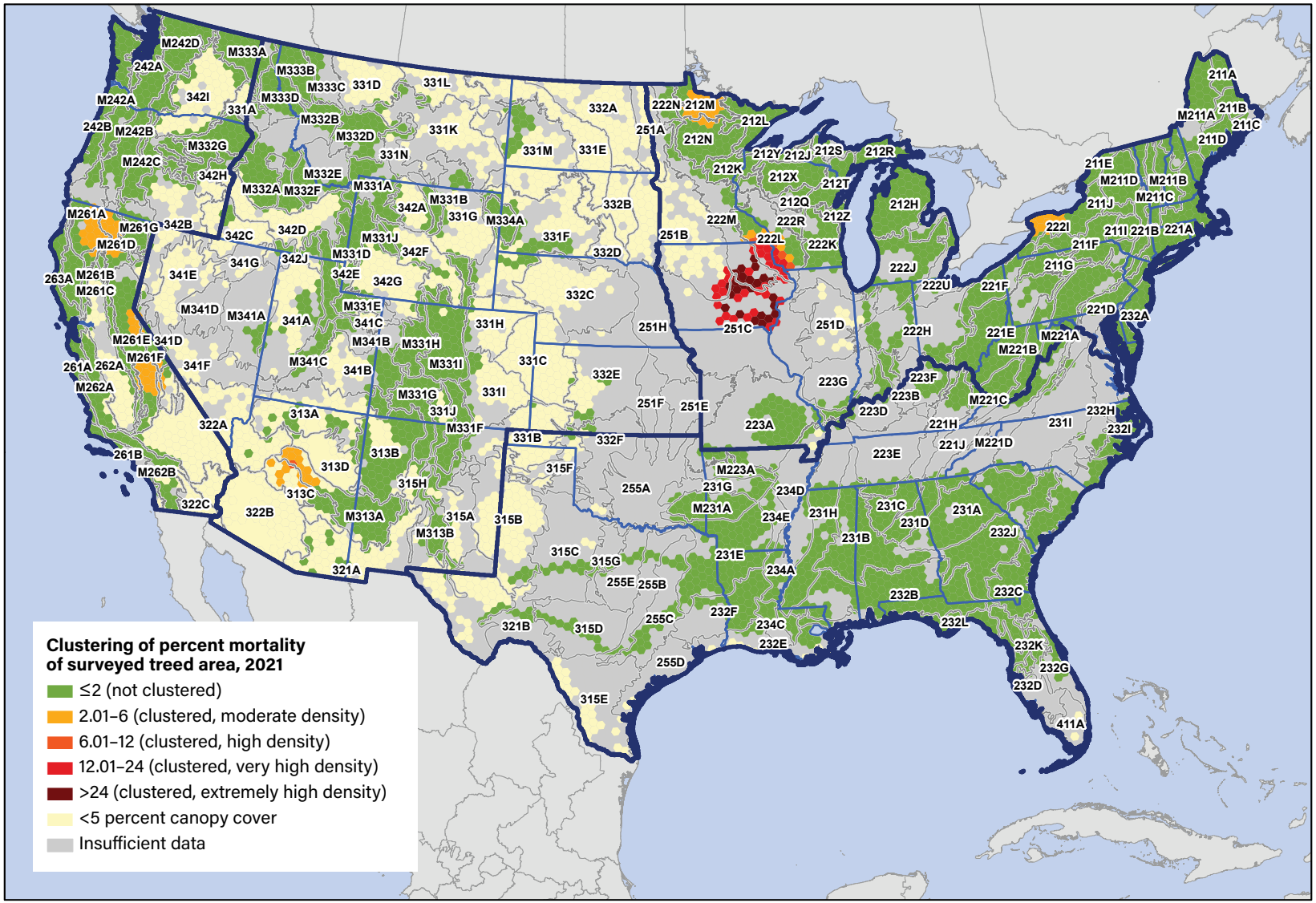

Figure 2.3—Hot spots of percentage of surveyed tree canopy cover area with insect and disease mortality in 2021 for the conterminous United States by hexagons containing >5-percent tree canopy cover. Values are Getis-Ord Gi* *scores, with values >2 representing significant clustering of high mortality occurrence densities and values <-2 representing significant clustering of low mortality occurrence densities. The gray lines delineate ecoregion sections (Cleland and others 2007), and blue lines delineate Forest Health Monitoring megaregions. Tree canopy cover is based on data from a cooperative project between the Multi-Resolution Land Characteristics Consortium (Coulston and others 2012) and the Forest Service Geospatial Technology and Applications Center using the 2011 National Land Cover Database. (Data source: U.S. Department of Agriculture, Forest Service, Forest Health Protection)*

M261G–Modoc Plateau (0.68 percent), and 341D–Mono (0.56 percent). California encompassed three hot spots of moderate mortality density, one in the northern part of the State and two in the Sierra Nevada (fig. 2.3).

Damage from 17 mortality agents and complexes was identified across 441 000 ha in the Interior West FHM megaregion in 2021 (table 2.3). The primary agent was the set of unknown bark beetles characterized as "Southwest bark beetle complex" in ponderosa pine forests, described above. This was associated with mortality on approximately 225 000 ha, or 51 percent of the total in the region. Other widespread agents were pinyon ips (*Ips confusus*) (66 000 ha, 15.1 percent), spruce beetle (*D. rufipennis*) (57 000 ha, 12.9 percent), Douglas-fir beetle (31 000 ha, 6.9 percent), and western balsam bark beetle (*Dryocoetes confusus*) (15 000 ha, 3.5 percent).

The Interior West ecoregion section with the highest mortality was 315A–Pecos Valley in east-central New Mexico (fig. 2.2), with mortality on 5.17 percent of surveyed tree canopy cover within the surveyed area. This mortality was associated with Southwest bark beetle complex, Douglas-fir beetle, and pinyon ips. These agents, along with fir engraver in white fir (*A. concolor*), were responsible for the relatively high levels of mortality in other ecoregion sections of the Southwest: 313C–Tonto Transition (1.56 percent), M313A–White Mountains-San Francisco Peaks-Mogollon Rim (0.93 percent), 313D–Painted Desert (0.75 percent), 313B–Navajo Canyonlands[1] (0.57 percent), and 313A–Grand Canyon (0.56 percent). A hot spot of moderate and high mortality densities occurred in M313A–White Mountains-San Francisco Peaks-Mogollon Rim and 313C–Tonto Transition (fig. 2.3).

Approximately 6500 ha in the Southern FHM megaregion had recorded damage from 12 mortality agents and complexes in 2021 (table 2.3). Ips engraver beetles represented the most widely detected agent, on 2800 ha or 44 percent of the total. The next two most widespread agents, the "unknown bark beetle" agent noted above and Douglas-fir beetle, caused damage in ponderosa pine forests of the Guadalupe Mountains of western Texas. As a result of these two agents, the 321A–Basin and Range ecoregion section of far-west Texas had 0.28-percent mortality of the surveyed tree canopy area (fig. 2.2).

Conterminous United States Defoliation

The national IDS in 2021 identified 56 defoliation agents and complexes affecting approximately 1.67 million ha within the area surveyed across the CONUS (table 2.4), which is almost equal to the land area of Hawaii. This is somewhat higher than in 2020, when defoliation across 1.54 million ha was attributed to 59 defoliating agents (Potter and Paschke 2022), although only about half as much area was surveyed in 2020. Spongy moth was the most widely detected defoliation agent in 2021, found on 1.02 million ha or 61.2 percent of the total defoliation area. This was a change from the previous 3 years, during which eastern spruce budworm was the most widely detected

[1] *This ecoregion section appears as 313B–Navaho Canyonlands in Cleland and others (2007).*

defoliation agent (Potter and Paschke 2022; Potter and others 2020b, 2021). In 2021, eastern spruce budworm was identified on about 183 000 ha, or 10.9 percent of the total. This was followed by western spruce budworm (*C. freemani*) on 172 000 ha (10.3 percent of the total). No other agents were detected on >100 000 ha, but browntail moth (*Euproctis chrysorrhoea*) (80 000 ha, 4.8 percent), which is currently only a problem in the coastal region of the Northeast, and Gelechiid moths/needleminers (*Coleotechnites* spp.) (41 000 ha, 2.4 percent) were relatively widespread.

The Eastern FHM megaregion had by far the largest area on which defoliation was detected in 2021, 1.36 million ha (table 2.5). Surveyors identified 33 defoliation agents in the surveyed area, with three-quarters of the defoliation area attributed to spongy moth (1.02 million ha). Other major defoliators were eastern spruce budworm (183 000 ha, 13.4 percent), browntail moth (80 000 ha, 5.8 percent), and locust leafminer (*Odontota dorsalis*) (21 000 ha, 1.6 percent).

As in 2020, two ecoregion sections in the Great Lakes area exceeded 5-percent defoliation of surveyed canopy cover (fig. 2.4): 212H–Northern Lower Peninsula of Michigan and 212L–Northern Superior Uplands in northeastern Minnesota. The defoliation in the Lower Peninsula was caused by spongy moth in hardwood forests, while the Northern Superior Uplands mortality was the result of eastern spruce budworm in fir and spruce forests. These ecoregions encompassed three hot spots of very high defoliation density (fig. 2.5).

Table 2.4—Defoliation agents and complexes affecting >5000 ha in the conterminous United States in 2021

Agents/complexes causing defoliation, 2021	Area (ha)[a]
Spongy moth	1 024 902
Eastern spruce budworm	183 159
Western spruce budworm	171 926
Browntail moth	79 587
Gelechiid moths/needleminers	40 509
Pinyon needle scale	22 587
Locust leafminer	21 168
Unknown	17 180
Balsam woolly adelgid	14 432
Unknown defoliator	14 073
Maple leafcutter	10 541
Douglas-fir tussock moth	10 390
Other defoliator, known (code pending)	8937
Fall cankerworm	8447
Large aspen tortrix	8079
Forest tent caterpillar	8014
Larch casebearer	5300
Other (39)	25 816
Total, all defoliation agents	1 673 020

[a] All values are "footprint" areas for each agent or complex. The sum of the individual agents is not equal to the total for all agents due to the reporting of multiple agents per polygon.

Table 2.5—The top five defoliation agents or complexes for each Forest Health Monitoring megaregion and for Alaska and Hawaii in 2021

Defoliation agents and complexes, 2021	Area (ha)[a]
Eastern	
Spongy moth	1 017 414
Eastern spruce budworm	183 159
Browntail moth	79 587
Locust leafminer	21 168
Maple leafcutter	10 541
Other defoliation agents (28)	51 102
Total, all defoliation agents and complexes	1 362 419
Interior West	
Western spruce budworm	171 926
Gelechiid moths/needleminers	40 509
Pinyon needle scale	22 587
Unknown defoliator	13 647
Douglas-fir tussock moth	5549
Other defoliation agents (6)	7215
Total, all defoliation agents and complexes	261 059
Southern	
Spongy moth	7487
Loblolly pine sawfly	3425
Other defoliator	458
Dothistroma needle blight (*D. pini*)	454
Unknown	27
Total, all defoliation agents and complexes	11 852

Defoliation agents and complexes, 2021	Area (ha)[a]
West Coast	
Balsam woolly adelgid	14 432
Unknown	10 900
Douglas-fir tussock moth	4841
Lodgepole needleminer	3440
Lodgepole sawfly	1290
Other defoliation agents (13)	3888
Total, all defoliation agents and complexes	37 690
Alaska	
Western blackheaded budworm	210 412
Aspen leafminer	59 163
Birch leafminer	19 307
Rusty tussock moth	17 855
Unknown defoliator	6917
Other defoliation agents (37)	5800
Total, all defoliation agents and complexes	314 219
Hawaii	
ʻŌhiʻa/guava rust	0
Total, all defoliation agents and complexes	0

[a] The total area affected by other agents is listed at the end of each section. All values are "footprint" areas for each agent or complex. The sum of the individual agents is not equal to the total for all agents due to the reporting of multiple agents per polygon.

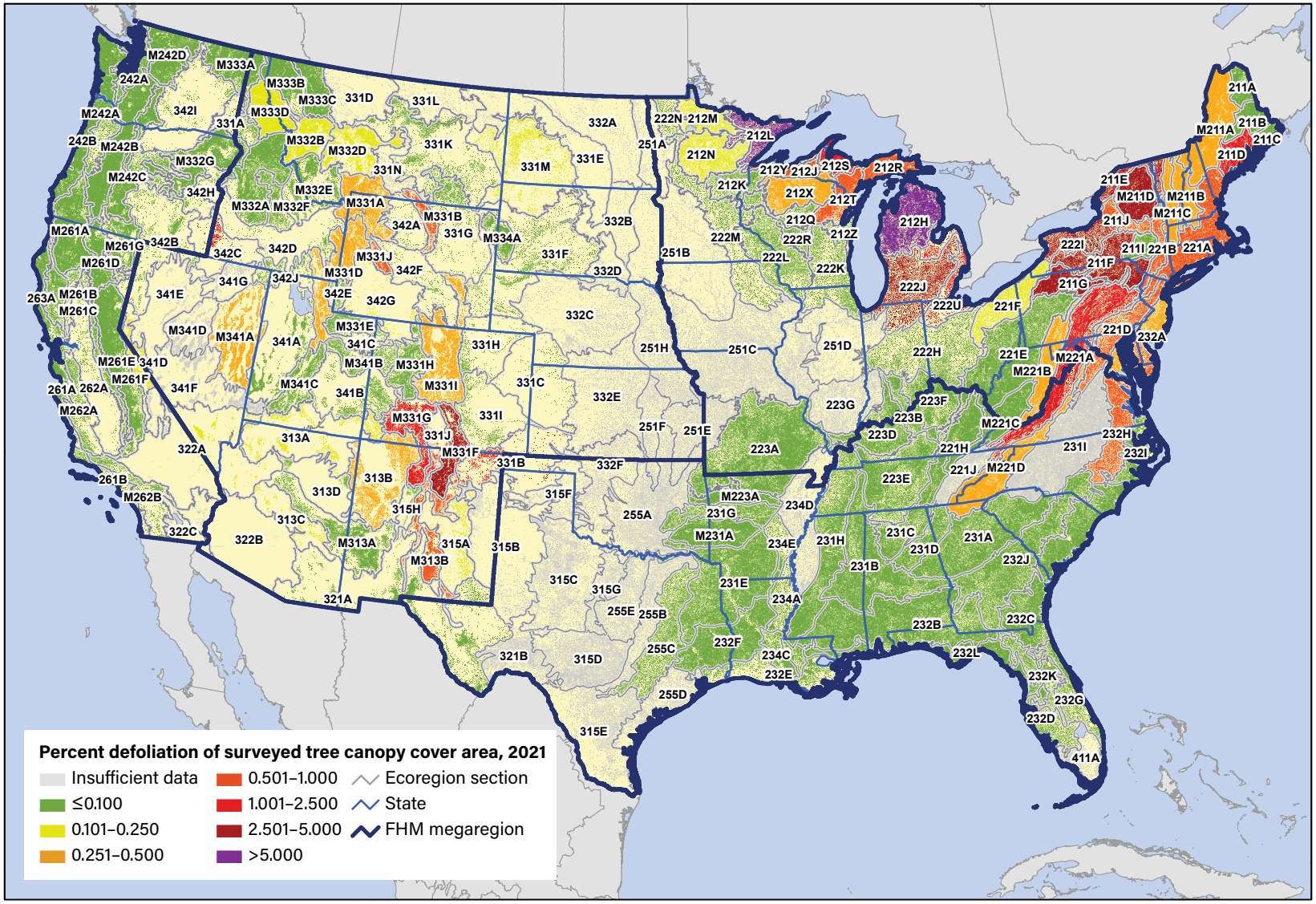

Figure 2.4—The percentage of surveyed tree canopy cover area with insect and disease defoliation, by ecoregion section within the conterminous United States, for 2021. The gray lines delineate ecoregion sections (Cleland and others 2007), and blue lines delineate Forest Health Monitoring megaregions. The 240-m tree canopy cover is based on data from a cooperative project between the Multi-Resolution Land Characteristics Consortium (Coulston and others 2012) and the Forest Service Geospatial Technology and Applications Center using the 2011 National Land Cover Database. (Data source: U.S. Department of Agriculture, Forest Service, Forest Health Protection)

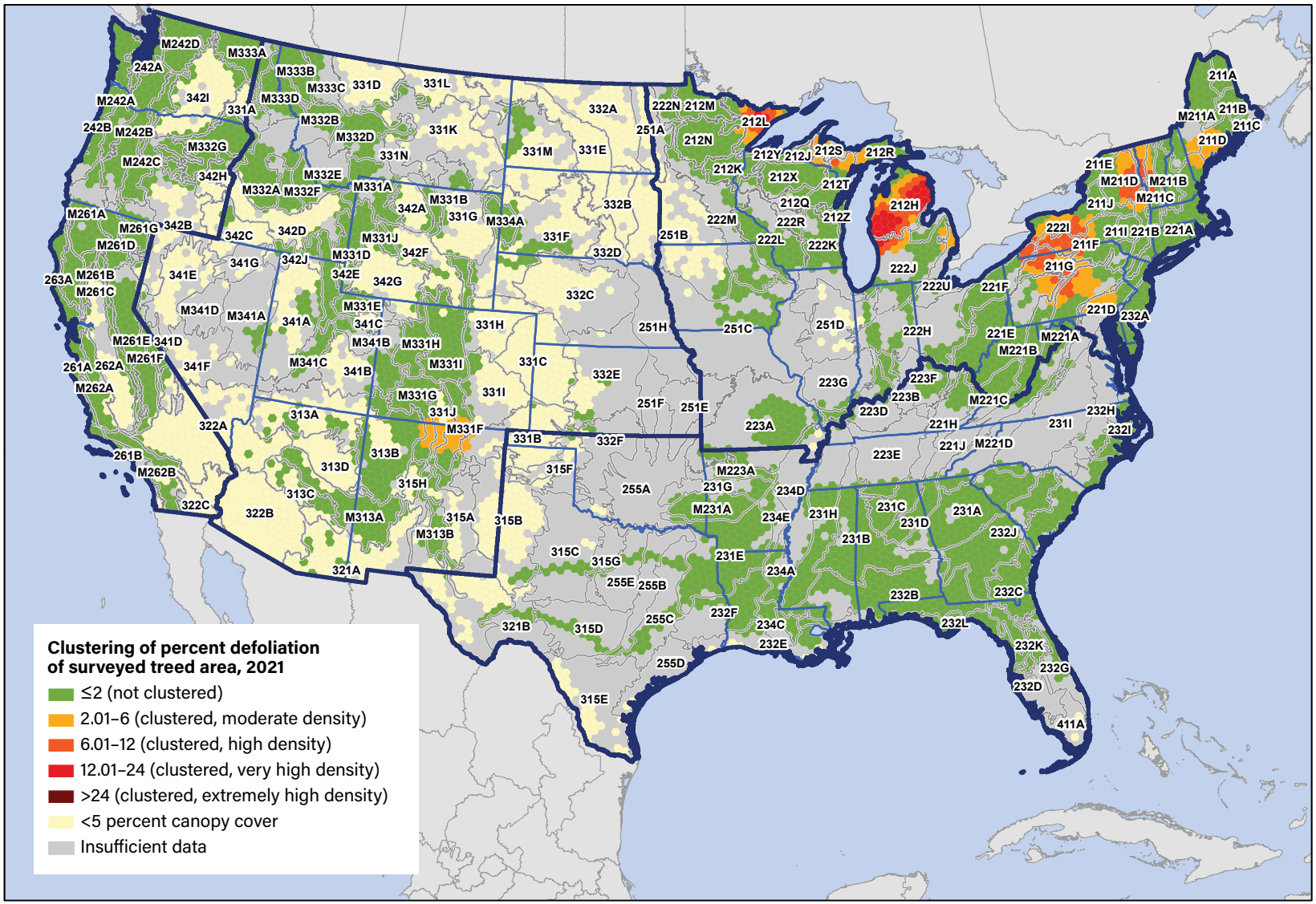

Figure 2.5—Hot spots of percentage of surveyed tree canopy cover area with insect and disease defoliation in 2021 for the conterminous United States by hexagons containing >5-percent tree canopy cover. Values are Getis-Ord Gi scores, with values >2 representing significant clustering of high defoliation occurrence densities. (No areas of significant clustering of low densities, <–2, were detected.) The gray lines delineate ecoregion sections (Cleland and others 2007), and blue lines delineate Forest Health Monitoring megaregions. Tree canopy cover is based on data from a cooperative project between the Multi-Resolution Land Characteristics Consortium (Coulston and others 2012) and the Forest Service Geospatial Technology and Applications Center using the 2011 National Land Cover Database. (Data source: U.S. Department of Agriculture, Forest Service, Forest Health Protection)*

The Eastern megaregion encompassed several other areas of high defoliation (>2.5 percent of surveyed canopy area). Several in New York and northern Pennsylvania were the result of spongy moth infestations (fig. 2.4):

- M211D–Adirondack Highlands (4.91-percent defoliation of surveyed canopy area)
- 211G–Northern Unglaciated Allegheny Plateau (4.85 percent)
- 211F–Northern Glaciated Allegheny Plateau (4.06 percent)
- 222I–Erie and Ontario Lake Plain (2.67 percent)
- 211E–St. Lawrence and Champlain Valley (2.66 percent)

These ecoregion sections were also the location of three hot spot areas of high defoliation density (fig. 2.5).

Farther west in the Great Lakes region, 2.88-percent defoliation in 222J–South Central Great Lakes on the Lower Peninsula of Michigan was caused by spongy moth, while the 2.75-percent defoliation of 212Y–Southwest Lake Superior Clay Plain (in northern Minnesota and Wisconsin and the Upper Peninsula of Michigan) was caused by large aspen tortrix (*Choristoneura conflictana*). Elsewhere, moderate levels of defoliation (1–2.5 percent) occurred in 212S–Northern Upper Peninsula (1.89 percent) because of an eastern spruce budworm outbreak, in 211D–Central Maine Coastal and Embayment (1.74 percent) because of a browntail moth infestation in northern red oak (*Quercus rubra*) stands, and in 222U–Lake Whittlesey Glaciolacustrine Plain (1.68 percent) and M221A–Northern Ridge and Valley (1.11 percent) because of spongy moth. All these areas had hot spots of at least moderate defoliation density (fig. 2.5).

In the Interior West FHM megaregion, 261 000 ha of damage in the surveyed area was attributed to 11 defoliators (table 2.5). As in recent years (Potter and Paschke 2022; Potter and others 2020b, 2021), western spruce budworm (172 000 ha) encompassed most of this area (65.9 percent). Gelechiid moths/needleminers were identified on 41 000 ha (15.5 percent), pinyon needle scale (*Matsucoccus acalyptus*) on 23 000 ha (8.7 percent), and Douglas-fir tussock moth (*Orgyia pseudotsugata*) on 6000 ha (2.1 percent).

The Interior West ecoregion section with the highest percent defoliation of surveyed canopy area (3.57 percent) was M331F–Southern Parks and Rocky Mountain Range, where outbreaks of Gelechiid moths/needleminers in ponderosa pine, western spruce budworm in fir and spruce, and an unknown defoliator in quaking aspen (*Populus tremuloides*) were detected (fig. 2.4). Meanwhile, western spruce budworm was the primary defoliation agent in the nearby M331G–South-Central Highlands ecoregion section (2.10-percent defoliation). Together, this damage caused a hot spot of moderate defoliation density in north-central New Mexico and south-central Colorado (fig. 2.5). Defoliation was also relatively high in M313B–Sacramento-Manzano Mountains to the south (0.77 percent), mostly because of pinyon needle scale.

Farther north, an outbreak of Douglas-fir tussock moth resulted in relatively high

defoliation (1.52 percent of surveyed canopy area) in 342C–Owyhee Highlands, while western spruce budworm was detected in M331J–Wind River Mountains (0.89 percent) and M331B–Bighorn Mountains (0.79 percent).

Meanwhile, 18 defoliating agents were recorded as affecting about 38 000 ha of surveyed area in the West Coast FHM megaregion during 2021 (table 2.5). Balsam woolly adelgid (*Adelges piceae*) was the most commonly detected, on 14 000 ha or 38.2 percent of all defoliation. An additional 11 000 ha of defoliation was attributed to an unknown defoliating agent (28.9 percent), while Douglas-fir tussock moth was detected on 4800 ha (12.8 percent) and lodgepole needleminer (*Coleotechnites milleri*) was found on 3400 ha (9.1 percent). No West Coast ecoregion section exceeded 1-percent defoliation of surveyed canopy area (fig. 2.4), and the megaregion did not encompass any defoliation hot spots (fig. 2.5).

In the Southern FHM megaregion, spongy moth (7500 ha, 63.1 percent of the total) was the most widely detected of five defoliation agents across 12 000 ha (table 2.5) within the surveyed area. Loblolly pine sawfly (*Neodiprion taedae linearis*) and Dothistroma needle blight (*Dothistroma pini*) were the other two identified defoliation agents, on 3400 ha and 500 ha, respectively (28.9 percent and 3.8 percent of defoliation area in the region). M221A–Northern Ridge and Valley in northern Virginia had 1.11-percent defoliation of the surveyed area (fig. 2.4) because of spongy moth detections. There were no defoliation hot spots in the megaregion (fig. 2.5).

Alaska and Hawaii

Surveyors detected 90 000 ha of mortality in Alaska in 2021 associated with nine agents (table 2.3), a slight increase in area from 2020. Spruce beetle, as in previous years, was the most widely detected mortality agent, representing 86.8 percent of the total for the State, across 78 000 ha. Two other mortality agents had a relatively extensive footprint, hemlock sawfly (*Neodiprion tsugae*), detected on 8500 ha (9.4 percent of the total), and yellow-cedar decline, identified on 3300 ha or 3.7 percent of the total.

As in 2020 (Potter and Paschke 2022), spruce beetle mortality was high in stands of white spruce (*Picea glauca*) in south-central Alaska (fig. 2.6), with extremely high 10.31-percent mortality across surveyed forest and shrubland in M133B–Alaska Range and a relatively high 2.58 percent in 133A–Cook Inlet Basin. M241C–Chugach-St. Elias Mountains also experienced spruce beetle mortality (0.31 percent). Meanwhile, mortality from hemlock sawfly in western hemlock (*Tsuga heterophylla*) stands and from yellow-cedar decline resulted in 0.15-percent mortality of the surveyed forest and shrubland of M241D–Alexander Archipelago in the Alaska panhandle.

Alaska experienced 314 000 ha of defoliation in 2021 (table 2.5), a considerable increase from the 68 000 ha detected in 2020 (Potter and Paschke 2022). This area was greater than any of the FHM regions in the CONUS except the Eastern, which experienced an extensive spongy moth outbreak. Of the 42 defoliating agents, western blackheaded budworm (*Acleris gloverana*) was the most

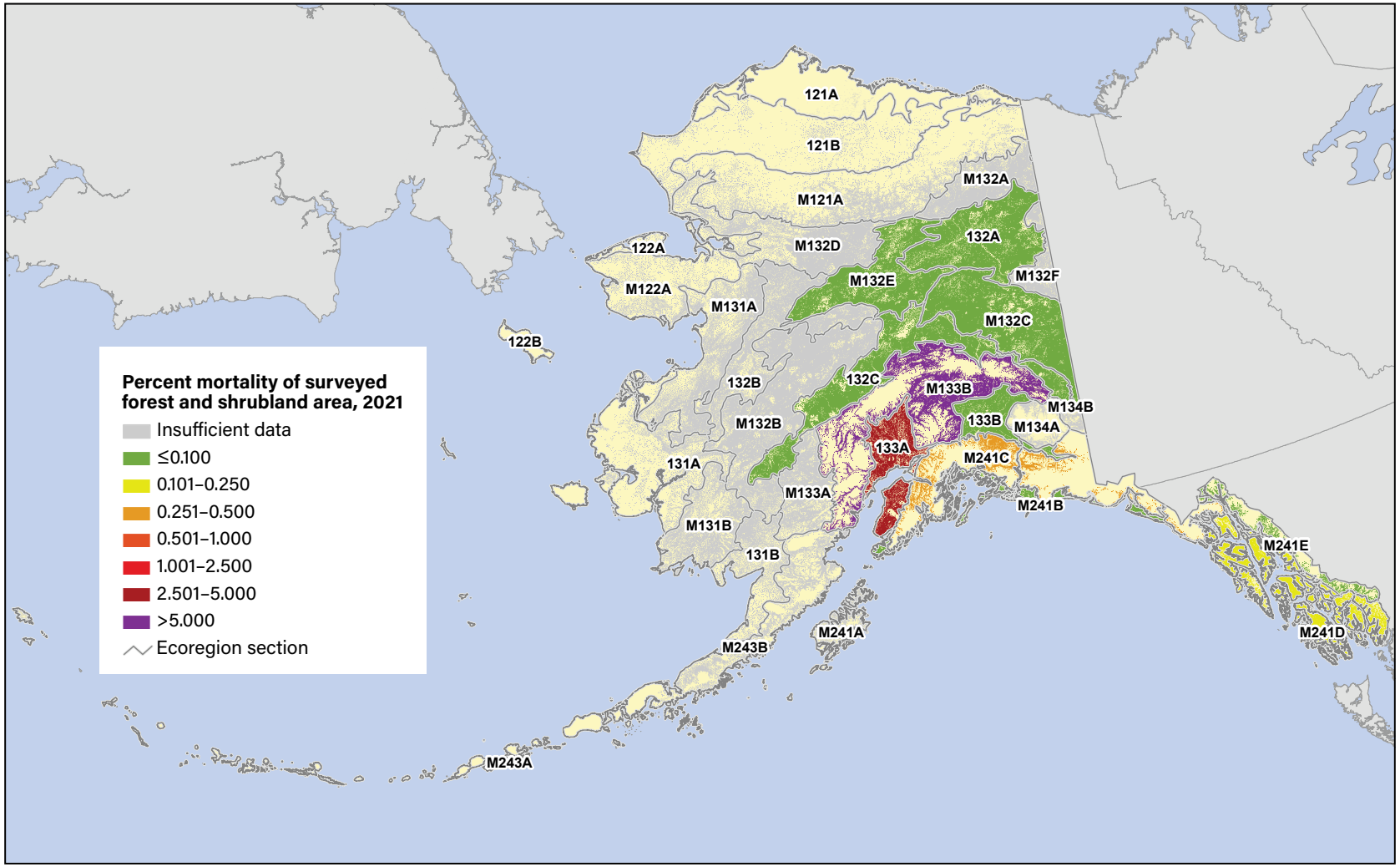

Figure 2.6—Percentage of 2021 surveyed Alaska forest and shrubland area within ecoregions with mortality caused by insects and diseases. The gray lines delineate ecoregion sections (Spencer and others 2002). Forest and shrub cover is derived from the 2011 National Land Cover Database. (Data source: U.S. Department of Agriculture, Forest Service, Forest Health Protection)

widely detected, on 210 000 ha, or 66.9 percent of the total defoliation area. Other widespread defoliators were aspen leafminer (*Phyllocnistis populiella*) on 59 000 ha (18.8 percent of the total), birch leafminer (*Fenusa pusilla*) on 19 000 ha (6.1 percent), and rusty tussock moth (*Orgyia antiqua*) on 18 000 ha (5.7 percent).

The highest levels of defoliation (5.03 percent of surveyed forest and shrubland) occurred in M241D–Alexander Archipelago in the Alaska panhandle, the location of a western blackheaded budworm outbreak in western hemlock (fig. 2.7). Four ecoregion sections in east-central Alaska had relatively high defoliation (>1 percent) because of activity by aspen leafminer, birch leafminer, and willow leaf blotchminer (*Micrurapteryx salicifoliella*):

- M132C–Yukon-Tanana Uplands (1.94 percent of surveyed forest and shrubland)
- M132E–Ray Mountains (1.49 percent)
- 132A–Yukon-Old Crow Basin (1.24 percent)
- 132C–Tanana-Kuskokwim Lowlands (1.15 percent).

Rusty tussock moth was the primary defoliator in M133B–Alaska Range (0.85-percent defoliation), while birch leafminer was detected in 133A–Cook Inlet Basin (0.35 percent).

Meanwhile, surveyors detected approximately 36 000 ha of mortality in Hawaii during 2021 (table 2.3), compared to 32 000 ha in 2020 (Potter and Paschke 2022) and 27 000 ha in 2019 (Potter and others 2021). While the mortality was not attributed to a specific agent, at least some of the damage was likely the result of rapid ʻōhiʻa death. This wilt disease is caused by two fungal pathogens, the more aggressive *Ceratocystis lukuohia* and the less aggressive *C. huliohia*, which both can kill ʻōhiʻa lehua (*Metrosideros polymorpha*) (Barnes and others 2018). This endemic species is the most abundant native tree in Hawaii, where it is deeply woven into Hawaiian culture (University of Hawaiʻi 2022). Both pathogens have been confirmed on Hawaiʻi Island, where most detections are of the more aggressive *C. lukuohia,* and on the island of Kauaʻi (University of Hawaiʻi 2022). In 2019, a small number of trees infected with *C. huliohia* were detected on Oʻahu and Maui, but it has not been detected on Maui since then (University of Hawaiʻi 2022).

Mortality was high across most of the montane wet ecoregions of Hawaiʻi Island, with extremely high mortality in Montane Wet-Hawaiʻi-Kaʻū (MWh-ka), where mortality was identified on 6.47 percent of the surveyed tree canopy area (fig. 2.8). Montane Wet-Hawaiʻi-Kona (MWh-ko) had 2.80-percent mortality, followed by Montane Wet-Hawaiʻi-Hilo-Puna (MWh-hp) (2.17 percent) and Montane Wet-Hawaiʻi-Kohala-Hāmākua (MWh-kh) (1.27 percent). There was 0.62-percent mortality of surveyed canopy area in the Mesic-Hawaiʻi ecoregion. High to moderate levels of mortality were also detected in three ecoregions on the island of Kauaʻi: Lowland Wet-Kauaʻi (LWk) (1.35 percent of surveyed tree canopy area), Montane Wet-Kauaʻi (MWk) (0.61 percent), and Mesic-Kauaʻi (MEk) (0.37 percent).

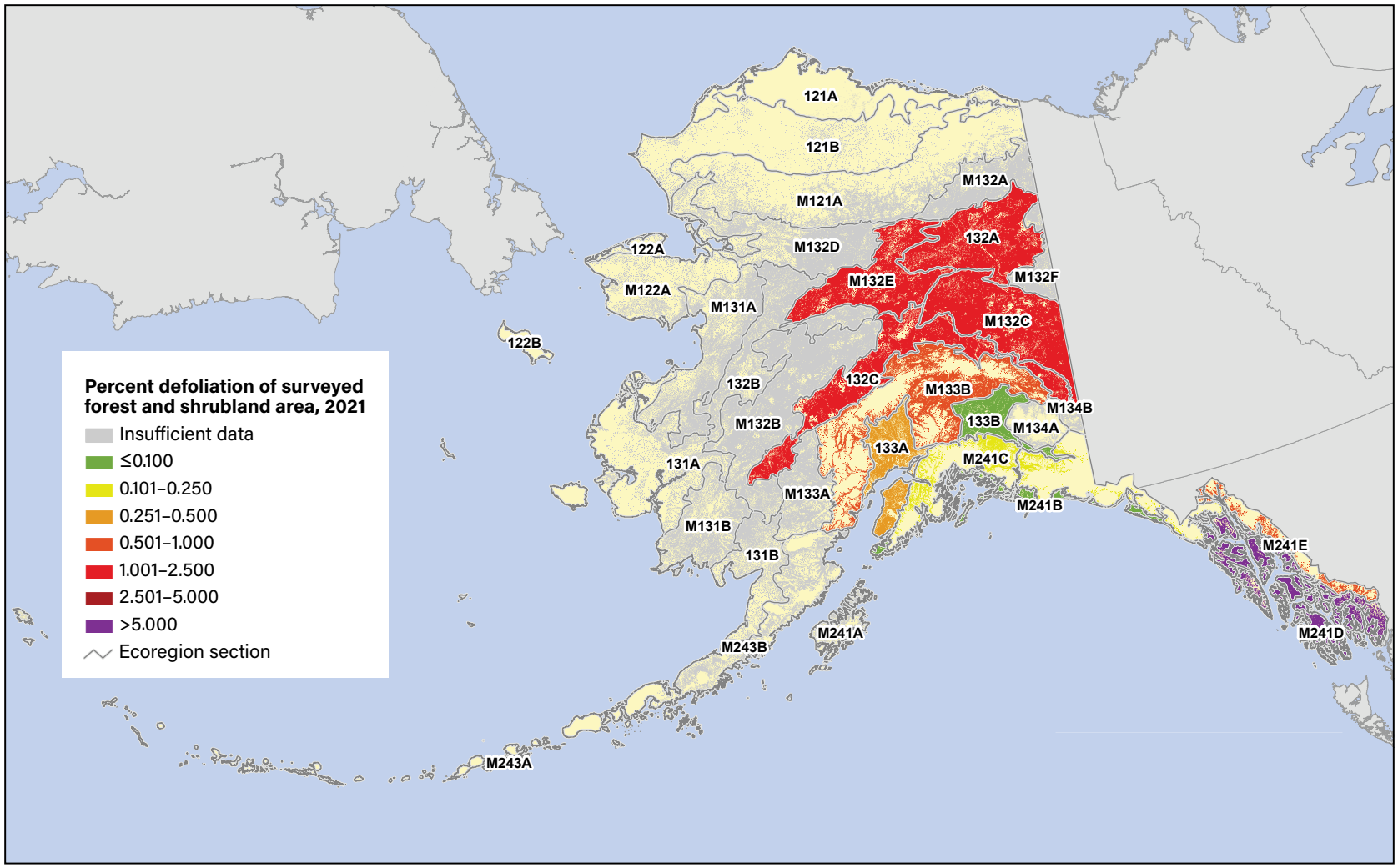

Figure 2.7—Percentage of 2021 surveyed Alaska forest and shrubland area within ecoregions with defoliation caused by insects and diseases. The gray lines delineate ecoregion sections (Spencer and others 2002). Forest and shrub cover is derived from the 2011 National Land Cover Database. (Data source: U.S. Department of Agriculture, Forest Service, Forest Health Protection)

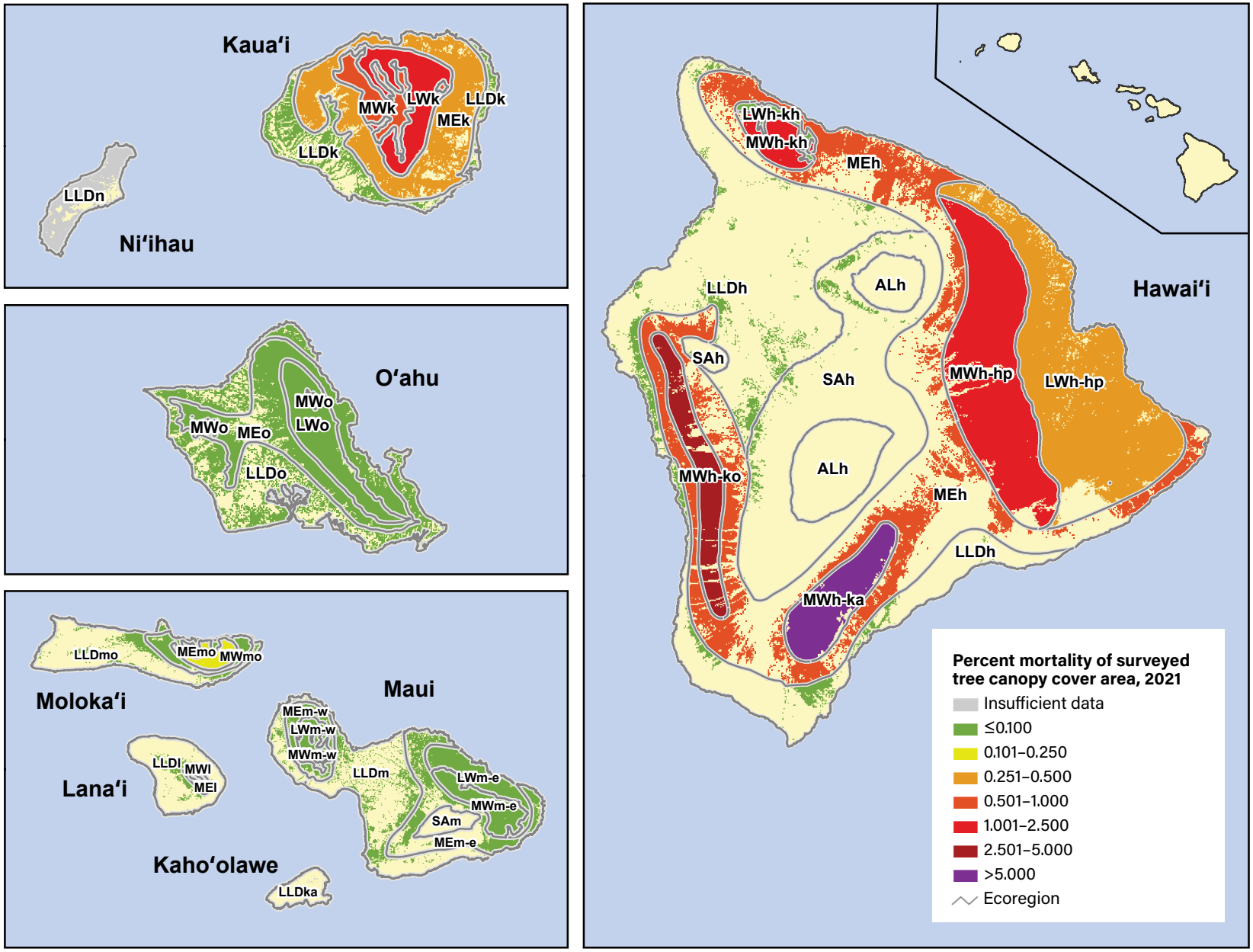

Figure 2.8—Percentage of 2021 surveyed Hawaii tree canopy area within island/ecoregion combinations with mortality caused by insects and diseases. Tree canopy cover is based on data from a cooperative project between the Multi-Resolution Land Characteristics Consortium (Coulston and others 2012) and the Forest Service Geospatial Technology and Applications Center using the 2011 National Land Cover Database. See table 1.1 for ecoregion identification. (Data source: U.S. Department of Agriculture, Forest Service, Forest Health Protection)

CONCLUSIONS

In 2021, forest health surveyors identified 60 mortality-causing agents and complexes across the CONUS on approximately 2.21 million ha, an area slightly less than the land area of New Hampshire. Emerald ash borer was the most widely detected mortality agent, identified on about 878 000 ha across the Eastern FHM megaregion, though mortality caused by this insect agent is challenging to map given the low density of ash in northern forests and other agents that also can cause ash mortality. This is consistent with recent years. Fir engraver caused extensive mortality in parts of the West, but the area of its impact has declined from recent years (e.g., Potter and others 2020b, 2021). As in recent years, Alaska experienced extensive mortality from spruce beetle, while much of the mortality in Hawaii may be associated with rapid ʻōhiʻa death.

Meanwhile, the national IDS reported damage in 2021 from 56 defoliation agents and complexes affecting approximately 1.67 million ha across the CONUS, almost equal to the land area of Hawaii. The majority of this defoliation was the result of a spongy moth outbreak, primarily in the Eastern FHM megaregion but in the Southern megaregion as well. Alaska had extensive defoliation, caused mostly by western blackheaded budworm in the Alexander Archipelago in the panhandle, as well as by aspen leafminer, birch leafminer, and rusty tussock moth in the interior of the State.

Continued monitoring of insect and disease outbreaks across the United States can guide appropriate follow-up investigation and management activities. Due to limitations of survey efforts to detect certain important forest insects and diseases, pests and pathogens discussed in this chapter do not include all the biotic forest health threats that are important to consider when making management decisions and budget allocations. However, large-scale assessments of mortality and defoliation severity represent a useful approach for identifying geographic areas where concentrations of monitoring and management activities might be most effective.

LITERATURE CITED

Abdulridha, J.; Ampatzidis, Y.; Ehsani, R.; de Castro, A. I. 2018. Evaluating the performance of spectral features and multivariate analysis tools to detect laurel wilt disease and nutritional deficiency in avocado. Computers and Electronics in Agriculture. 155: 203–211. https://doi.org/10.1016/j.compag.2018.10.016.

Anselin, L. 1992. Spatial data analysis with GIS: an introduction to application in the social sciences. Tech. Rep. 92-10. Santa Barbara, CA: National Center for Geographic Information and Analysis. 53 p.

Barnes, I.; Fourie, A.; Wingfield, M.J. [and others]. 2018. New Ceratocystis species associated with rapid death of *Metrosideros polymorpha* in Hawaii. Persoonia-Molecular Phylogeny and Evolution of Fungi. 40(1): 154–181. https://doi.org/10.3767/persoonia.2018.40.07.

Berryman, E.; McMahan, A. 2019. Using tree canopy cover data to help estimate acres of damage. In: Potter, K.M.; Conkling, B.L., eds. Forest Health Monitoring: national status, trends, and analysis 2018. Gen. Tech. Rep. SRS-239. Asheville, NC: U.S. Department of Agriculture, Forest Service, Southern Research Station: 125–141.

Brockerhoff, E.G.; Liebhold, A.M.; Jactel, H. 2006. The ecology of forest insect invasions and advances in their management. Canadian Journal of Forest Research. 36(2): 263–268. https://doi.org/10.1139/x06-013.

Castello, J.D.; Leopold, D.J.; Smallidge, P.J. 1995. Pathogens, patterns, and processes in forest ecosystems. BioScience. 45(1): 16–24. https://doi.org/10.2307/1312531.

Cleland, D.T.; Freeouf, J.A.; Keys, J.E. [and others]. 2007. Ecological subregions: sections and subsections for the conterminous United States. Gen. Tech. Rep. WO-76D. Washington, DC: U.S. Department of Agriculture, Forest Service. Map; Sloan, A.M., cartographer; presentation scale 1:3,500,000; colored. https://doi.org/10.2737/WO-GTR-76D.

Coleman, T.W.; Graves, A.D.; Heath, Z. [and others]. 2018. Accuracy of aerial detection surveys for mapping insect and disease disturbances in the United States. Forest Ecology and Management. 430: 321–336. https://doi.org/10.1016/j.foreco.2018.08.020.

Coulston, J.W.; Moisen, G.G.; Wilson, B.T. [and others]. 2012. Modeling percent tree canopy cover: a pilot study. Photogrammetric Engineering and Remote Sensing. 78(7): 715–727. https://doi.org/10.14358/PERS.78.7.715.

Edmonds, R.L.; Agee, J.K.; Gara, R.I. 2011. Forest health and protection. Long Grove, IL: Waveland Press, Inc. 667 p.

ESRI. 2017. ArcMap® 10.5.1. Redlands, CA: Environmental Systems Research Institute.

Forest Health Protection (FHP). 2019. Digital Mobile Sketch Mapping user's manual 2.1. Fort Collins, CO: U.S. Department of Agriculture, Forest Service, Forest Health Assessment and Applied Sciences Team. https://www.fs.usda.gov/foresthealth/technology/docs/DMSM_Tutorial/story_content/external_files/DMSM_User_Guide.pdf. [Date accessed: August 10, 2022].

Forest Health Protection (FHP). 2022. Insect and Disease Detection Survey (IDS) data downloads. Fort Collins, CO: U.S. Department of Agriculture, Forest Service, Forest Health Technology Enterprise Team. https://www.fs.usda.gov/foresthealth/applied-sciences/mapping-reporting/detection-surveys.shtml. [Date accessed: August 10, 2022].

Getis, A.; Ord, J.K. 1992. The analysis of spatial association by use of distance statistics. Geographical Analysis. 24(3): 189–206. https://doi.org/10.1111/j.1538-4632.1992.tb00261.x.

Hanavan, R.P.; Pontius, J.; Hallett, R. 2015. A 10-year assessment of hemlock decline in the Catskill Mountain region of New York State using hyperspectral remote sensing techniques. Journal of Economic Entomology. 108(1): 339–349. https://doi.org/10.1093/jee/tou015.

Hanavan, R.P.; Kamoske, A.G.; Schaaf, A.N. [and others]. 2021. Supplementing the Forest Health National Aerial Survey Program with remote sensing during the COVID-19 pandemic: lessons learned from a collaborative approach. Journal of Forestry. 2021: 1–8. https://doi.org/10.1093/jofore/fvab056.

Holdenrieder, O.; Pautasso, M.; Weisberg, P.J.; Lonsdale, D. 2004. Tree diseases and landscape processes: the challenge of landscape pathology. Trends in Ecology & Evolution. 19(8): 446–452. https://doi.org/10.1016/j.tree.2004.06.003.

Homer, C.G.; Dewitz, J.A.; Yang, L. [and others]. 2015. Completion of the 2011 National Land Cover Database for the conterminous United States: representing a decade of land cover change information. Photogrammetric Engineering and Remote Sensing. 81(5): 345–354.

Laffan, S.W. 2006. Assessing regional scale weed distributions, with an Australian example using *Nassella trichotoma*. Weed Research. 46(3): 194–206. https://doi.org/10.1111/j.1365-3180.2006.00491.x.

Liebhold, A.M.; McCullough, D.G.; Blackburn, L.M. [and others]. 2013. A highly aggregated geographical distribution of forest pest invasions in the USA. Diversity and Distributions. 19: 1208–1216. https://doi.org/10.1111/ddi.12112.

Logan, J.A.; Regniere, J.; Powell, J.A. 2003. Assessing the impacts of global warming on forest pest dynamics. Frontiers in Ecology and the Envionment. 1: 130–137. https://doi.org/10.1890/1540-9295(2003)001[0130:ATIOGW]2.0.CO;2.

Lovett, G.M.; Weiss, M.; Liebhold, A.M. [and others]. 2016. Nonnative forest insects and pathogens in the United States: impacts and policy options. Ecological Applications. 26: 1437–1455. https://doi.org/10.1890/15-1176.

Mack, R.N.; Simberloff, D.; Lonsdale, W.M. [and others]. 2000. Biotic invasions: causes, epidemiology, global consequences, and control. Ecological Applications. 10(3): 689–710. https://doi.org/10.1890/1051-0761(2000)010[0689:BICEGC]2.0.CO;2.

Manion, P.D. 2003. Evolution of concepts in forest pathology. Phytopathology. 93: 1052–1055. https://doi.org/10.1094/PHYTO.2003.93.8.1052.

Parry, D.; Teale, S.A. 2011. Alien invasions: the effects of introduced species on forest structure and function. In: Castello, J.D.; Teale, S.A., eds. Forest health: an integrated perspective. New York: Cambridge University Press: 115–162. https://doi.org/10.1017/CBO9780511974977.006.

Pontius, J.; Hanavan, R.P.; Hallett, R.A. [and others]. 2017. High spatial resolution spectral unmixing for mapping ash species across a complex urban environment. Remote Sensing of Environment. 199: 360–369. https://doi.org/10.1016/j.rse.2017.07.027.

Potter, K.M. 2012. Large-scale patterns of insect and disease activity in the conterminous United States and Alaska from the national Insect and Disease Detection Survey database, 2007 and 2008. In: Potter, K.M.; Conkling, B.L., eds. Forest Health Monitoring 2009 national technical report. Gen. Tech. Rep. SRS-167. Asheville, NC: U.S. Department of Agriculture, Forest Service, Southern Research Station: 63–78.

Potter, K.M. 2013. Large-scale patterns of insect and disease activity in the conterminous United States and Alaska from the national Insect and Disease Detection Survey, 2009. In: Potter, K.M.; Conkling, B.L., eds. Forest Health Monitoring: national status, trends, and analysis 2010. Gen. Tech. Rep. SRS-176. Asheville, NC: U.S. Department of Agriculture, Forest Service, Southern Research Station: 15–29.

Potter, K.M. 2023. Ecological regions of Hawai'i. Fort Collins, CO: Forest Service Research Data Archive. https://doi.org/10.2737/RDS-2023-0018. [Date accessed: July 31, 2023].

Potter, K.M.; Canavin, J.C.; Koch, F.H. 2020a. A forest health retrospective: national and regional results from 20 years of Insect and Disease Survey data. In: Potter, K.M.; Conkling, B.L., eds. Forest Health Monitoring: national status, trends, and analysis 2019. Gen. Tech. Rep. SRS-250. Asheville, NC: U.S. Department of Agriculture, Forest Service, Southern Research Station: 125–149.

Potter, K.M.; Escanferla, M.E.; Jetton, R.M.; Man, G. 2019a. Important insect and disease threats to United States tree species and geographic patterns of their potential impacts. Forests. 10(4): 304. https://doi.org/10.3390/f10040304.

Potter, K.M.; Escanferla, M.E.; Jetton, R.M. [and others]. 2019b. Prioritizing the conservation needs of United States tree species: evaluating vulnerability to forest insect and disease threats. Global Ecology and Conservation. 18: e00622. https://doi.org/10.1016/j.gecco.2019.e00622.

Potter, K.M.; Koch, F.H. 2012. Large-scale patterns of insect and disease activity in the conterminous United States and Alaska, 2006. In: Potter, K.M.; Conkling, B.L., eds. Forest Health Monitoring 2008 national technical report. Gen. Tech. Rep. SRS-158. Asheville, NC: U.S. Department of Agriculture, Forest Service, Southern Research Station: 63–72.

Potter, K.M.; Koch, F.H.; Oswalt, C.M.; Iannone, B.V. 2016. Data, data everywhere: detecting spatial patterns in fine-scale ecological information collected across a continent. Landscape Ecology. 31: 67–84. https://doi.org/10.1007/s10980-015-0295-0.

Potter, K.M.; Paschke, J.L. 2013. Large-scale patterns of insect and disease activity in the conterminous United States and Alaska from the national Insect and Disease Detection Survey database, 2010. In: Potter, K.M.; Conkling, B.L., eds. Forest Health Monitoring: national status, trends, and analysis 2011. Gen. Tech. Rep. SRS-185. Asheville, NC: U.S. Department of Agriculture, Forest Service, Southern Research Station: 15–28.

Potter, K.M.; Paschke, J.L. 2014. Large-scale patterns of insect and disease activity in the conterminous United States and Alaska from the national Insect and Disease Survey database, 2011. In: Potter, K.M.; Conkling, B.L., eds. Forest Health Monitoring: national status, trends, and analysis 2012. Gen. Tech. Rep. SRS-198. Asheville, NC: U.S. Department of Agriculture, Forest Service, Southern Research Station: 19–34.

Potter, K.M.; Paschke, J.L. 2015a. Large-scale patterns of insect and disease activity in the conterminous United States and Alaska from the national Insect and Disease Survey, 2012. In: Potter, K.M.; Conkling, B.L., eds. Forest Health Monitoring: national status, trends, and analysis 2013. Gen. Tech. Rep. SRS-207. Asheville, NC: U.S. Department of Agriculture, Forest Service, Southern Research Station: 19–36.

Potter, K.M.; Paschke, J.L. 2015b. Large-scale patterns of insect and disease activity in the conterminous United States, Alaska, and Hawaii from the national Insect and Disease Survey, 2013. In: Potter, K.M.; Conkling, B.L., eds. Forest Health Monitoring: national status, trends, and analysis 2014. Gen. Tech. Rep. SRS-209. Asheville, NC: U.S. Department of Agriculture, Forest Service, Southern Research Station: 19–38.

Potter, K.M.; Paschke, J.L. 2016. Large-scale patterns of insect and disease activity in the conterminous United States and Alaska from the national Insect and Disease Survey, 2014. In: Potter, K.M.; Conkling, B.L., eds. Forest Health Monitoring: national status, trends, and analysis 2015. Gen. Tech. Rep. SRS-213. Asheville, NC: U.S. Department of Agriculture, Forest Service, Southern Research Station: 21–40.

Potter, K.M.; Paschke, J.L. 2017. Large-scale patterns of insect and disease activity in the conterminous United States and Alaska from the national Insect and Disease Survey, 2015. In: Potter, K.M.; Conkling, B.L., eds. Forest Health Monitoring: national status, trends, and analysis 2016. Gen. Tech. Rep. SRS-222. Asheville, NC: U.S. Department of Agriculture, Forest Service, Southern Research Station: 21–42.

Potter, K.M.; Paschke, J.L. 2022. Broad-scale patterns of insect and disease activity across the 50 United States from the national Insect and Disease Survey, 2020. In: Potter, K.M.; Conkling, B.L., eds. Forest Health Monitoring: national status, trends, and analysis, 2021. Gen. Tech. Rep. SRS-266. Asheville, NC: U.S. Department of Agriculture, Forest Service, Southern Research Station: 25–49. https://doi.org/10.2737/SRS-GTR-266-Chap2.

Potter, K.M.; Paschke, J.L.; Koch, F.H.; Berryman, E.M. 2020b. Large-scale patterns of insect and disease activity in the conterminous United States, Alaska, and Hawaii from the national Insect and Disease Survey, 2018. In: Potter, K.M.; Conkling, B.L., eds. Forest Health Monitoring: national status, trends, and analysis 2019. Gen. Tech. Rep. SRS-250. Asheville, NC: U.S. Department of Agriculture, Forest Service, Southern Research Station: 27–55.

Potter, K.M.; Paschke, J.L.; Koch, F.H.; Zweifler, M. 2019c. Large-scale patterns of insect and disease activity in the conterminous United States, Alaska, and Hawaii from the national Insect and Disease Survey, 2017. In: Potter, K.M.; Conkling, B.L., eds. Forest Health Monitoring: national status, trends, and analysis 2018. Gen. Tech. Rep. SRS-239. Asheville, NC: U.S. Department of Agriculture, Forest Service, Southern Research Station: 21–49.

Potter, K.M.; Paschke, J.L.; Berryman, E.M. 2021. Large-scale patterns of insect and disease activity in the conterminous United States, Alaska, and Hawaii from the national Insect and Disease Survey, 2019. In: Potter, K.M.; Conkling, B.L., eds. Forest Health Monitoring: national status, trends, and analysis 2020. Gen. Tech. Rep. SRS-261. Asheville, NC: U.S. Department of Agriculture, Forest Service, Southern Research Station: 27–57.

Potter, K.M.; Paschke, J.L.; Zweifler, M. 2018. Large-scale patterns of insect and disease activity in the conterminous United States, Alaska, and Hawaii from the national Insect and Disease Survey, 2016. In: Potter, K.M.; Conkling, B.L., eds. Forest Health Monitoring: national status, trends, and analysis 2017. Gen. Tech. Rep. SRS-233. Asheville, NC: U.S. Department of Agriculture, Forest Service, Southern Research Station: 23–44.

Reams, G.A.; Smith, W.D.; Hansen, M.H. [and others]. 2005. The Forest Inventory and Analysis sampling frame. In: Bechtold, W.A.; Patterson, P.L., eds. The enhanced Forest Inventory and Analysis program—national sampling design and estimation procedures. Asheville, NC: U.S. Department of Agriculture, Forest Service, Southern Research Station: 11–26.

Shima, T.; Sugimoto, S.; Okutomi, M. 2010. Comparison of image alignment on hexagonal and square lattices. In: 2010 IEEE international conference on image processing. [Place of publication unknown]: Institute of Electrical and Electronics Engineers, Inc.: 141–144. https://doi.org/10.1109/icip.2010.5654351.

Slaton, M.R.; Warren, K.; Koltunov, A.; Smith, S. 2021. Accuracy assessment of Insect and Disease Survey and eDART for monitoring forest health. In: Potter, K.M.; Conkling, B.L., eds. Forest Health Monitoring: national status, trends, and analysis 2020. Gen. Tech. Rep. SRS-261. Asheville, NC: U.S. Department of Agriculture, Forest Service, Southern Research Station: 187–195.

Spencer, P.; Nowacki, G.; Fleming, M. [and others]. 2002. Home is where the habitat is: an ecosystem foundation for wildlife distribution and behavior. Arctic Research of the United States. 16: 6–17.

Teale, S.A.; Castello, J.D. 2011. Regulators and terminators: the importance of biotic factors to a healthy forest. In: Castello, J.D.; Teale, S.A., eds. Forest health: an integrated perspective. New York: Cambridge University Press: 81–114. https://doi.org/10.1017/CBO9780511974977.005.

Tobin, P.C. 2015. Ecological consequences of pathogen and insect invasions. Current Forestry Reports. 1: 25–32. https://doi.org/10.1007/s40725-015-0008-6.

University of Hawai'i, College of Tropical Agriculture and Human Resources. 2022. Rapid 'ōhi'a death. http://rapidohiadeath.org. [Date accessed: July 12, 2022].

White, D.; Kimerling, A.J.; Overton, W.S. 1992. Cartographic and geometric components of a global sampling design for environmental monitoring. Cartography and Geographic Information Systems. 19(1): 5–22. https://doi.org/10.1559/152304092783786636.

Zhang, L.; Rubin, B.D.; Manion, P.D. 2011. Mortality: the essence of a healthy forest. In: Castello, J.D.; Teale, S.A., eds. Forest health: an integrated perspective. New York: Cambridge University Press: 17–49. https://doi.org/10.1017/CBO9780511974977.003.